

~~RESTRICTED~~

UNCLASSIFIED

COPY NO. 7

RM E9B01

RM 9B01
NACA

Inactive

~~CONFIDENTIAL~~



~~36-35~~
Address 8-35/1
123
copy 2

RESEARCH MEMORANDUM

PERFORMANCE OF J33 TURBOJET ENGINE WITH
SHAFT-POWER EXTRACTION

III - TURBINE PERFORMANCE

By M. C. Huppert and J. C. Nettles

Lewis Flight Propulsion Laboratory
Cleveland, Ohio

CLASSIFIED - UNCANCELLED

Authority ~~20-16501-2843~~ Date 11/30/57

By ~~20-16501-12/9/57~~ See

CLASSIFICATION CHANGED

To: ~~Confidential~~
20-16501-1 Rel. form # 16-48
By authority of: ~~to: General~~ 94-12/1/5

REVIEWED BUT NOT
EDITED

CLASSIFIED DOCUMENT

This document contains classified information affecting the National Defense of the United States within the meaning of the Espionage Act, USC 50-31 and 52. Its transmission or the revelation of its contents in any manner to an unauthorized person is prohibited by law. Information so classified may be imparted only to persons in the military and naval services of the United States, appropriate civilian officers and employees of the Federal Government who have a legitimate interest therein, and to United States citizens of known loyalty and discretion who of necessity must be informed thereof.

NATIONAL ADVISORY COMMITTEE FOR AERONAUTICS

WASHINGTON

June 6, 1949

UNCLASSIFIED

~~RESTRICTED~~
~~CONFIDENTIAL~~



NATIONAL ADVISORY COMMITTEE FOR AERONAUTICS

RESEARCH MEMORANDUM

PERFORMANCE OF J33 TURBOJET ENGINE WITH SHAFT-POWER EXTRACTION

III - TURBINE PERFORMANCE

By M. C. Huppert and J. C. Nettles

SUMMARY

The performance of the turbine component of a J33 turbojet engine was determined over a range of turbine speeds from 8000 to 11,500 rpm. Turbine-inlet temperature was varied from the minimum required to drive the compressor to a maximum of approximately 2000° R at each of several intermediate turbine speeds.

Data are presented that show the horsepower developed by the turbine per pound of gas flow. The relation between turbine-inlet stagnation pressure, turbine-outlet stagnation pressure, and turbine-outlet static pressure was established. The turbine-weight-flow parameter varied from 39.2 to 43.6. The maximum turbine efficiency measured was 0.86 at a pressure ratio of 3.5 and a ratio of blade speed to theoretical nozzle velocity of 0.39. A generalized performance map of the turbine-horsepower parameter plotted against the turbine-speed parameter indicated that the best turbine efficiency is obtained when the turbine power is 10 percent greater than the compressor horsepower. The variation of efficiency with the ratio of blade speed to nozzle velocity indicated that the turbine operates at a speed above that for maximum efficiency when the engine is operated normally with the 19-inch-diameter jet nozzle.

INTRODUCTION

The performance of any @s-turbine unit is determined to a large extent by the air-flow capacity and efficiency of the components. The minimum specific fuel consumption for any combination of components is achieved when all the components are operating at the maximum efficiency obtainable at the desired power-output condition. In order to evaluate adequately the performance of a turbine and to determine if it is operating at maximum efficiency, the power output of the turbine must be varied at each operating speed.

The power developed by the turbine of a conventional turbojet engine for any given rotational speed is **equal**, except during transient **conditions**, to that required to drive the **compressor** plus that **required** to drive the engine **accessories**.

As part of a general analysis of the performance of a **turbine-propeller engine**, an investigation **was** conducted at the **NACA** Lewis laboratory on a **J33** turbojet engine in order to determine the shaft horsepower available as well as the performance **characteristics** of the engine components. The shaft **power** available maybe **used for** a number of purposes such as driving a propeller or driving engine **accessory** pumps. In this investigation, the engine was considered as a turbine-propeller **engine**.

The data were obtained by **so** attaching a dynamometer to the engine that shaft horsepower could be extracted. The over-all engine performance is presented in reference 1 and the performance characteristics of the compressor component are presented in reference 2. This report presents the performance characteristics of the turbine component.

APPARATUS AND PROCEDURE

Turbine

The 533 turbine **is** of partial-reaction **design**, having 48 **stator** blades **and** 54 rotor blades. The over-all turbine diameter is 26 inches and the **stator** and rotor blades are 4 inches long. A diagrammatic **sketch** showing the arrangement **of** the nozzle and the rotor blades is shown **in** figure 1. The nozzle area of the turbine investigated is 0.84 square foot and the ratio of turbine-nozzle area to turbine-outlet **annulus** area **is** 0.426. **The** angles between blade camber lines at the pitch section and the axial plane of the turbine are: **stator** outlet, **62°**; rotor inlet, **24°**; and rotor outlet, **47°**.

The turbine **exhausts** into a diffusing section having an inlet-outlet area ratio **of** 0.82 and an outlet diameter of 21 inches.

Installation and **Experimental** Procedure

The turbine was **investigated** as a component of a **J33** Jet engine, which was directly coupled to an induction-brake dynamometer and mounted on a **bedplate** suspended on cables. **This** suspension afforded **direct** measurement of Jet thrust by means of a strain-gage weighing device developed by the **NACA**.

The Jet-nozzle **size** was altered to change the turbine-outlet Static pressure **and** to increase the **range of** turbine operation **with** Shaft-power extraction. Three ratios of turbine-nozzle **area** to jet-nozzle area were used: 0.426 obtained **with a 19-inch-diameter** nozzle; 0.365, with 8 **20-inch** nozzle; and 0.350, **with a 21-inch** nozzle. At **each** of sever81 **speeds**, the turbine-inlet **temperature** was varied from the minimum required to drive the compressor to a **maximum** of **approximately 2000° R.**

The **equations** used to calculate temperature, gas flow, and efficiency and definitions of all symbols **used are** given in the appendix.

Instrumentation

The **engine was** instrumented to **obtain gas temperatures** and **pressures** at the stations shown in figure 2. Station 1 is at the **compressor inlet**, station 2 at the **compressor** outlet, station 3 at the **turbine inlet**, station 4 at the turbine outlet, and **station 5** at the turbine-diffuser outlet. At station 2, **alternate air** adapters contained **iron-constantan** thermocouples **and pitot** tubes so **located in the air stream as to** measure **representative values of** temperature and pressure. The thermocouples were of the bare-wire type without radiation **shields and the pitot** tube conformed to A.S.M.E. **standards.** **Pitot** tubes were **installed** at each of the burner outlets for measurement of pressures **at station 3.** Four wafer-type **static-pressure taps** were installed at station 4, **as shown in figure 1.** The **instrumentation at station 5 consisted** of 2 Static-pressure tubes, 2 **stagnation-pressure tubes**, and 14 unshielded **bare-wire** thermocouples.

Fuel flow to the engine **was** measured by a calibrated rotameter. Power output of the turbine **was** determined on the **basis of unit** gas flow through the turbine by **means** of calculations based on the measured **temperature rise** of the compressor, the dynamometer power, and the weight of gas flow.

RESULTS AND DISCUSSION

Turbine-power output. - Curves of equivalent turbine **horse-**
power per pound of gas flow $\frac{P_t}{W_g \theta_3}$ as a function of turbine-inlet-
temperature correction factor θ_3 at various engine **speeds are**
shown in figure 3 for the **20-inch-diameter** Jet nozzle. Over the

range investigated, $\frac{P_4}{W_g \theta_3}$ increases with engine speed and is nearly independent of turbine-inlet temperature. The changes in turbine-inlet pressure and in turbine efficiency apparently counteract each other.

Turbine pressure ratio. - It can be shown analytically that a turbine having a fixed nozzle area and a fixed exhaust area immediately downstream of the rotor (station 4) has a relation between inlet stagnation pressure p'_3 , outlet static pressure p_4 , and diffuser-outlet stagnation pressure p'_5 that is represented by a single curve. Figure 4 is a plot of the turbine stagnation-pressure ratio p'_3/p'_5 as a function of the ratio of inlet stagnation to outlet static pressure p'_3/p_4 . A curve is also shown giving the condition for maximum turbine stagnation pressure ratio that occurs when the velocity at Station 4 becomes sonic. The maximum stagnation-pressure ratio of 2.42 occurred at a value of p'_3/p_4 of 4.5, at which point the turbine was choked at station 4.

Turbine-power-extraction effectiveness. - The effectiveness of the turbine in terms of the ratio of power actually extracted from the fluid to the maximum power that could be extracted if the fluid left the turbine at zero velocity can be calculated from p'_3 , p'_4 , and p_4 . The variation of turbine-power-extraction effectiveness (actual horsepower/ideal horsepower $\times \eta'$, or η/η') with p'_3/p_4 is shown in figure 5. The turbine-power-extraction effectiveness decreased from 0.745 at a p'_3/p_4 of 2.0 to 0.635 at a p'_3/p_4 of 4.5.

Turbine-weight-flow parameter. - A plot of generalized turbine-weight-flow parameter $\frac{W_g \sqrt{\theta_3}}{\delta_3 \frac{\gamma}{1.4}}$ as a function of the ratio of turbine-inlet stagnation pressure to turbine-diffuser-outlet static pressure, p'_3/p_5 , is shown in figure 6. The maximum theoretical value of the flow parameter, based on a flow area of 0.84 square foot is shown as a line at 41.5. The total variation of $\frac{W_g \sqrt{\theta_3}}{\delta_3 \frac{\gamma}{1.4}}$ was from 39.2 to 43.6.

In figure 7, $\frac{W_g \sqrt{\theta_3}}{\delta_3 \frac{\gamma}{1.4}}$ is plotted against turbine-inlet temperature. In general, $\frac{W_g \sqrt{\theta_3}}{\delta_3 \frac{\gamma}{1.4}}$ increases with an increase in

turbine-inlet temperature. The over-all spread of the data, however, is such that the trend of the flow parameter with turbine-inlet temperature is inconclusive.

Turbine adiabatic efficiency. - The variation of adiabatic efficiency η' with the ratio of blade speed to theoretical turbine-nozzle velocity U/V at several values of p'_3/p_4 is shown in figure 8. Blade speed is based on the wheel diameter at the blade pitch diameter end nozzle velocity is based on p'_3 , T'_3 and p_4 . The maximum value of η' occurred at a value of U/V of about 0.39 for all values of p'_3/p_4 . As p'_3/p_4 increased, maximum efficiency increased from 0.816 at a pressure ratio of 2.0 to 0.863 at a pressure ratio of 3.5 and then decreased to 0.844 at a pressure ratio of 4.0. Inasmuch as p'_5 used for calculation of the turbine efficiency was measured at the outlet of the turbine-diffusing section (station 5), the pressure losses of the diffuser are included in the turbine losses. The characteristics of the diffuser have an unknown influence on the efficiency plots of figure 8. The range of U/V through which the turbine operates at sea-level static conditions with a 19-inch-diameter Jet nozzle is represented by a dashed line in figure 8. The position of the line indicates that the normal speed of the turbine is too high for maximum efficiency.

Performance characteristic curves. - Performance characteristic curves of the turbine in terms of horsepower per pound of gas flow $\frac{P_t}{W_g \theta_3}$ and equivalent engine speed $N/\sqrt{\theta_3}$ are shown in figure 9.

Contours of constant efficiency and constant turbine pressure ratio are presented for the range of engine operation from zero shaft power (turbine power equals compressor power) to a shaft power equal to 30 percent of the compressor power. This plot indicates that for jet-engine conditions at a given speed the turbine operates at a power output below that for maximum efficiency. It can be seen that the best efficiency condition occurs when the turbine power is 10 percent greater than the compressor power. The trends of turbine performance in figures 8 and 9 indicate that far jet-engine operation a better matching between the turbine and the compressor could be achieved by so increasing the amount of reaction in the turbine blades that the effective U/V would be reduced without reducing turbine power.

SUMMARY OF RESULTS

The performance of the turbine component of a J33 jet engine was determined over a range of turbine speeds between 8000 and 11,500 rpm. Turbine-inlet temperature was varied from the minimum required to drive the compressor to a maximum of about 2000° R. From this investigation, the following results were obtained:

1. The equivalent turbine horsepower per pound of gas flow increased with operating speed but was practically independent of turbine-inlet temperature over the range tested.
2. Throughout the entire range of operation, the relation between the ratio of inlet stagnation pressure to outlet static pressure and the ratio of inlet stagnation pressure to outlet stagnation pressure was represented by a single curve. A maximum stagnation-pressure ratio of 2.42 occurred at a ratio of inlet stagnation pressure to outlet static pressure of 4.5, at which point the turbine was choked at the outlet annulus.
3. The effectiveness of turbine-power extraction decreased from 0.745 at a ratio of inlet stagnation pressure to outlet static pressure of 2.0 to 0.635 at a pressure ratio of 4.5. For the range investigated, the turbine-weight-flow parameter varied from 39.2 to 43.6.
4. In general, the turbine-weight-flow parameter increased with increase in turbine-inlet temperature, although the trend was inconclusive.
5. The variation of efficiency with the ratio of blade speed to nozzle velocity indicated that the turbine operates at a speed above that for maximum efficiency when the engine is operated normally with the 19-inch-diameter Jet nozzle. The generalized performance characteristic curves indicated that the best turbine efficiency occurs when the turbine power is 10 percent greater than the compressor power. The maximum turbine efficiency measured was 0.86 at a pressure ratio of 3.5 and a ratio of blade speed to theoretical nozzle velocity of 0.39.

Lewis Flight Propulsion Laboratory,
National Advisory Committee for Aeronautics,
Cleveland, Ohio.

APPENDIX - CALCULATIONS OF TEMPERATURE, GAS FLOW, AND EFFICIENCY

Symbols

The following symbols and values are used in this report:

- A area, sq ft
- c_p specific heat of gas at constant pressure, Btu/(lb)(°R)
- c_v specific heat of gas at constant volume, Btu/(lb)(°R)
- g acceleration due to gravity, 32.2 ft/sec
- J mechanical equivalent of heat, 778 ft-lb/Btu
- K correction factor for gas flow, 0.81
- N engine speed, rpm
- P_s shaft horsepower (absorbed by dynamometer)
- P_t turbine horsepower
- p static pressure, lb/sq in. absolute
- p' stagnation pressure, lb/sq in. absolute
- R gas constant, 53.4 ft-lb/(lb)(°F)
- T static temperature, °R
- T' stagnation temperature, °R
- U velocity of turbine blade at pitch line, ft/sec
- V theoretical turbine-nozzle velocity based on value of inlet stagnation pressure to outlet static pressure,

$$\sqrt{2Jgc_p T'_3 \left[1 - \left(\frac{p_4}{p'_3} \right)^{\frac{\gamma-1}{\gamma}} \right]}$$
, ft/sec
- W weight flow, lb/sec
- γ ratio of specific heats, c_p/c_v

- 8** ratio of stagnation pressure to **NACA** standard atmospheric pressure, $p'/14.7$
 η adiabatic efficiency (based on **stagnation-to-static** pressure ratio)
 η' **adiabatic** efficiency (based on **stagnation pressure** ratio)
 θ ratio of **stagnation** temperature to **NACA** standard sea-level temperature multiplied by average ratio of specific heats of process divided by 1.4, $\left(\frac{T'}{518.4}\right)\left(\frac{\gamma_t}{1.4}\right)$

Subscripts:

- 1** **compressor** inlet
2 **compressor** outlet
3 **turbine** inlet
4 turbine outlet
5 turbine-diffuser outlet
c **compressor**
g **gas**
i indicated
t turbine

Calculations

The following equations are used in the calculations:

Static temperature,

$$T_5 = \frac{T'_{1,5}}{1 + 0.6 \left[\left(\frac{p'_{1,5}}{p_5} \right)^{\frac{\gamma_5 - 1}{\gamma_5}} - 1 \right]} \quad (1)$$

Stagnation temperature,

$$T'_{1,5} = T_5 \left(\frac{p'_{1,5}}{p_5} \right)^{\frac{\gamma_5 - 1}{\gamma_5}} \quad (2)$$

Turbine-inlet stagnation temperature,

$$T'_{3} = T'_{5} + \frac{\gamma_c (\gamma_t - 1)}{(\gamma_c - 1) \gamma_t} (T'_2 - T'_1) + \frac{(\gamma_t - 1) 550 P_g}{W_g R \gamma_t} \quad (3)$$

Tail-pipe gas flow,

$$W_g = 144 K p_5 A_4 \sqrt{\frac{2g\gamma_5}{R(\gamma_5 - 1)}} \sqrt{\frac{\left[\left(\frac{p'_5}{p_5} \right)^{\frac{\gamma_5 - 1}{\gamma_5}} - 1 \right] \left\{ 1 + 0.6 \left[\left(\frac{p'_5}{p_5} \right)^{\frac{\gamma_5 - 1}{\gamma_5}} - 1 \right] \right\}}{T'_{1,5}}} \quad (4)$$

Turbine efficiency,

$$\eta'_t = \frac{1 - \frac{T'_5}{T'_3}}{1 - \left(\frac{p'_5}{p'_3} \right)^{\frac{\gamma_t - 1}{\gamma_t}}} \quad (5)$$

REFERENCES

1. Nettles, J. C., and Esterly, J. R.: Performance of J33 Turbojet Engine with Shaft-Power Extraction. 3 - Over-All Engine Performance. NACA RM E8B27a, 1948.
2. Ross, Albert O., Esterly, John R., and Nettles, J. Cary: Performance of J33 Turbojet Engine with Shaft Power Extraction. II - Compressor. NACA RM E8B27b, 1948.

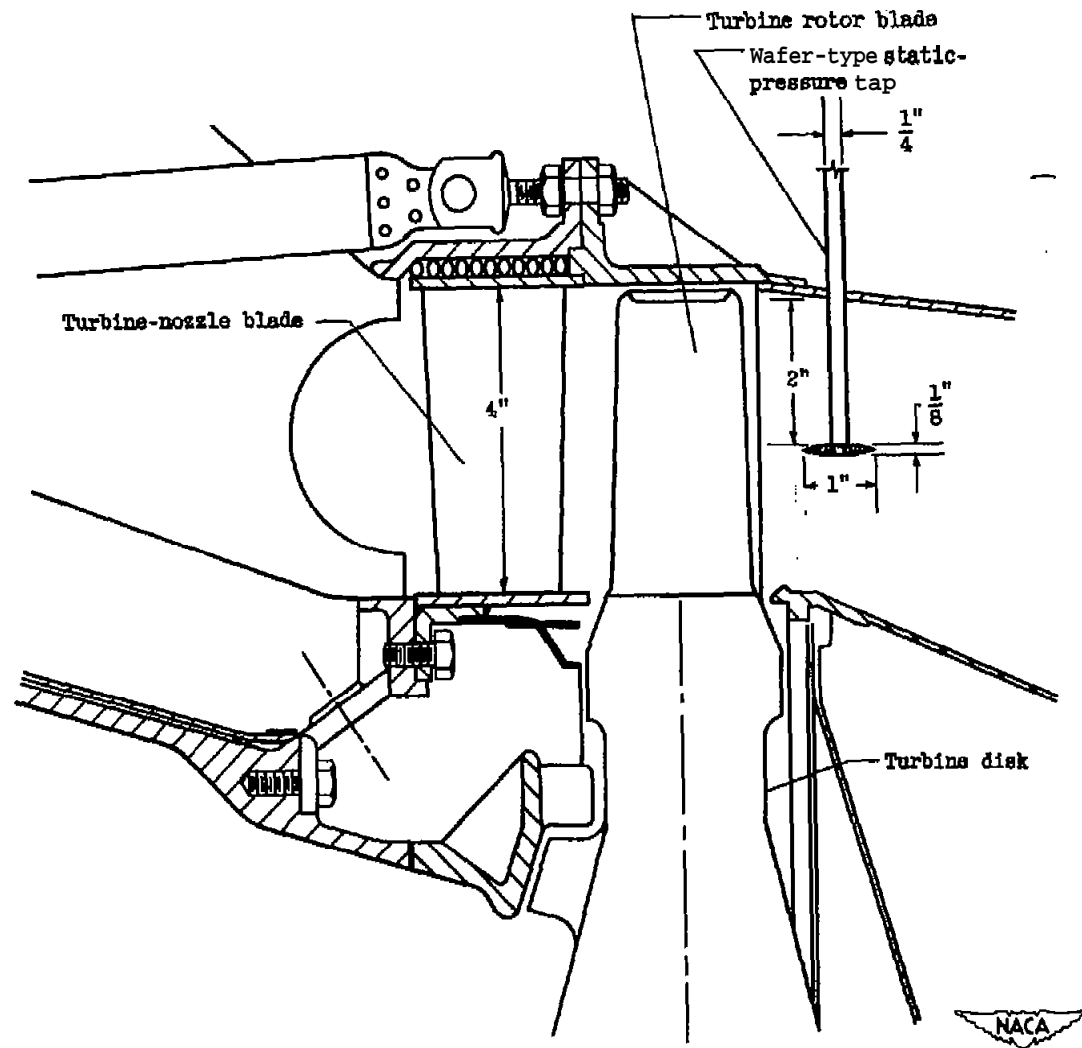


Figure 1. - Diagrammatic sketch of nozzle and rotor blades in turbine.

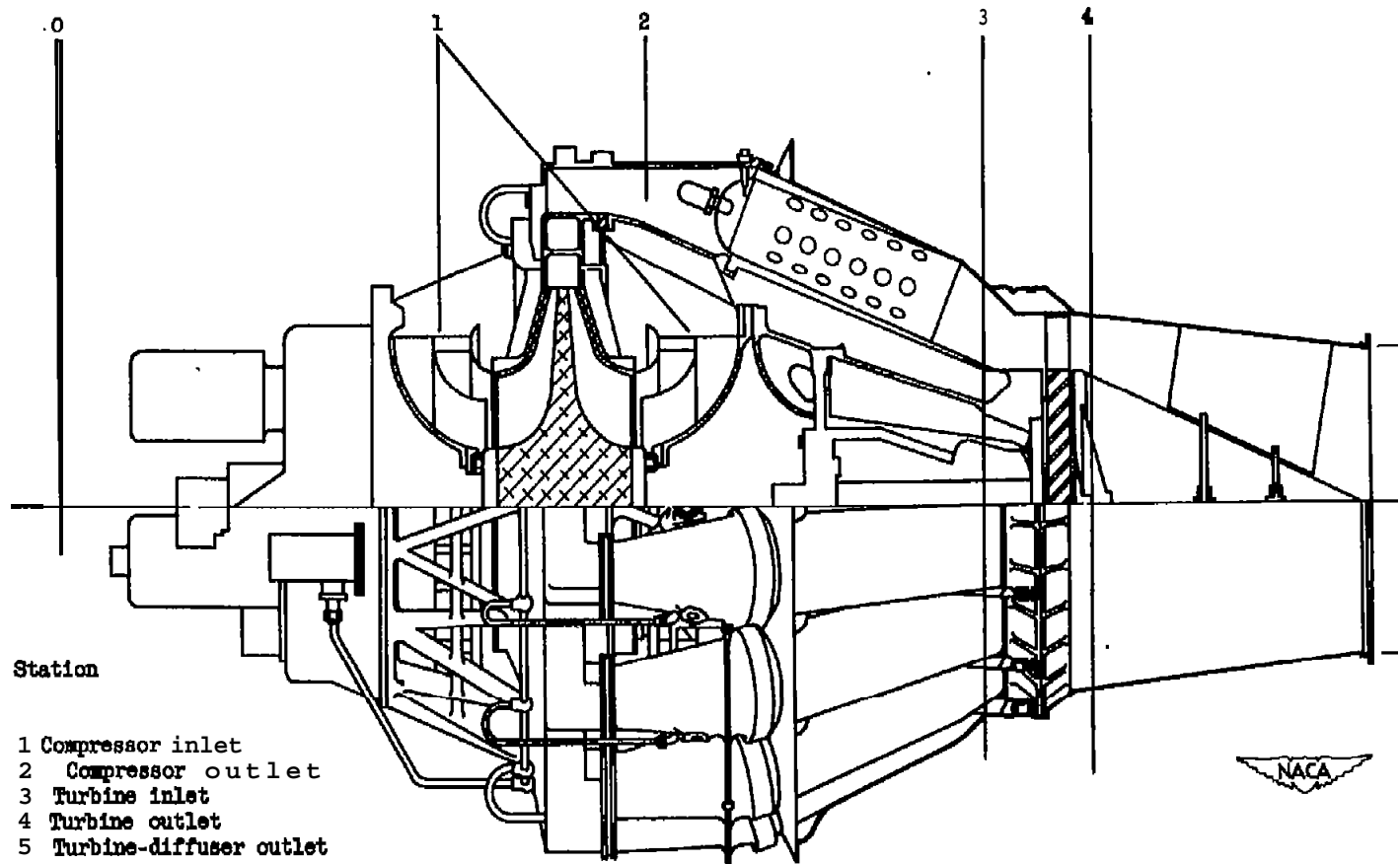


Figure 2. - Cross section of J33 engine showing instrumentation stations.

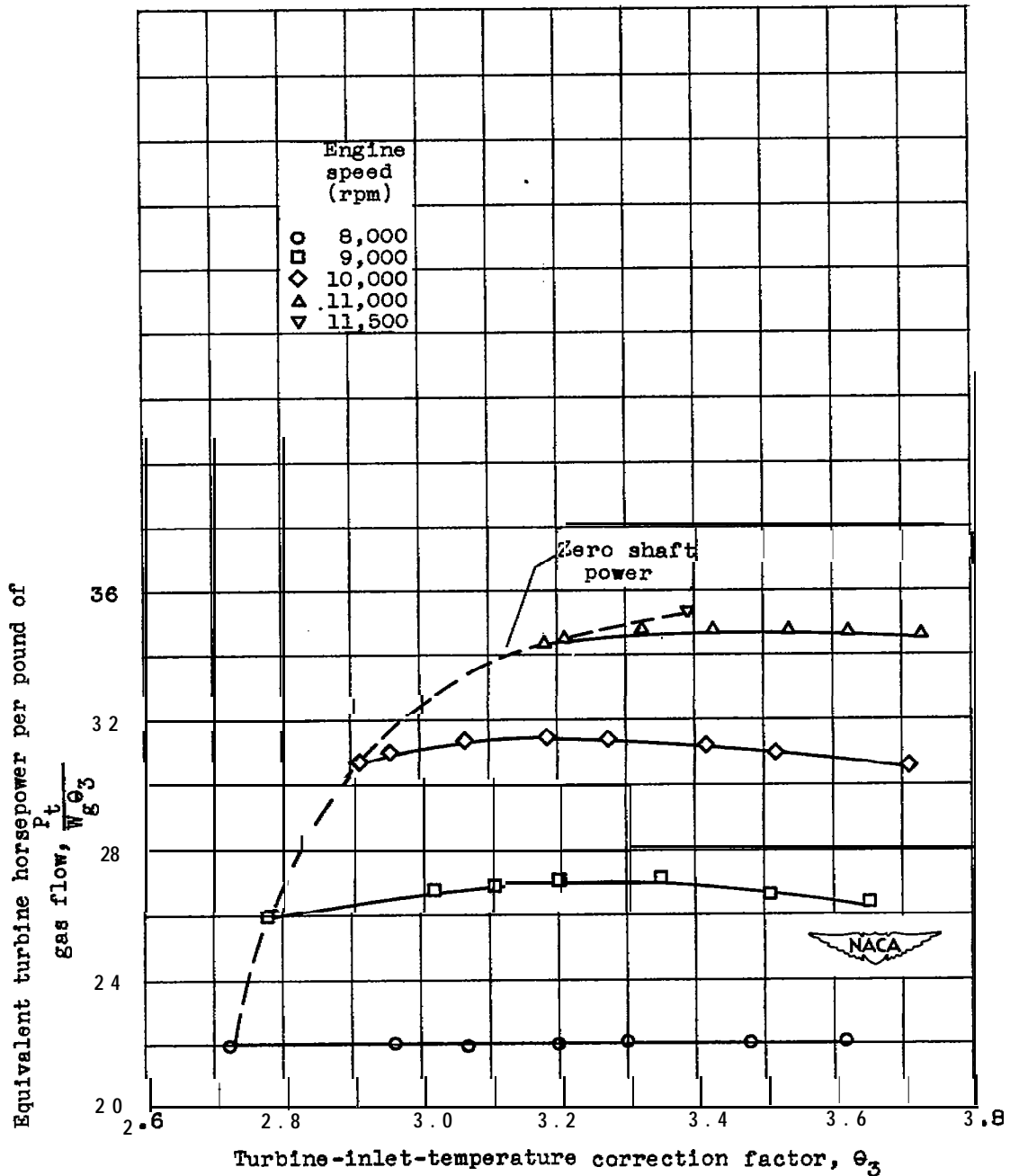


Figure 3. - Variation of equivalent turbine horsepower per pound of gas with temperature correction factor. Jet-nozzle diameter, 2.0 inches.

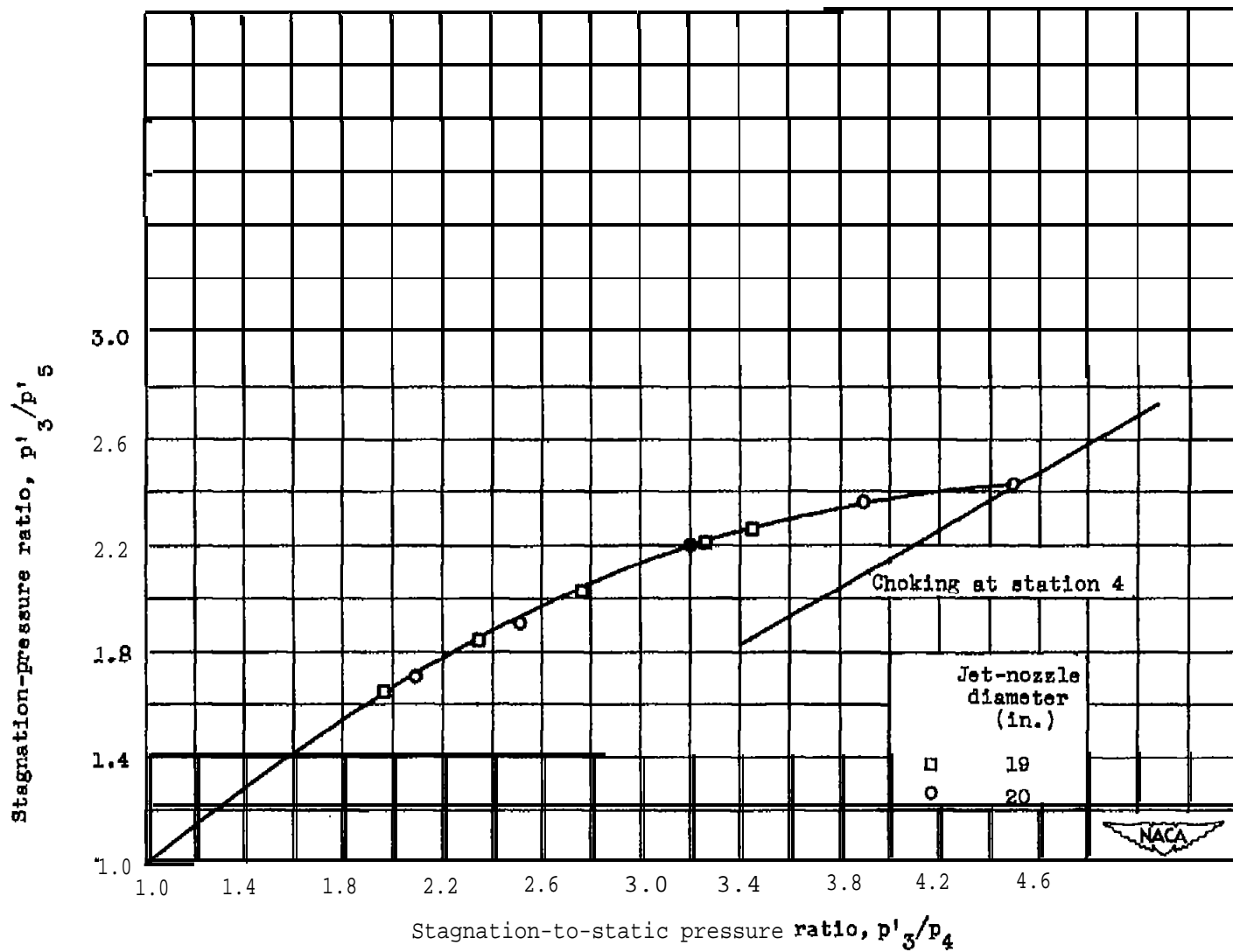


Figure 4. - Relation between stagnation-to-static and stagnation pressure ratios.
Shaft horsepower, 0.

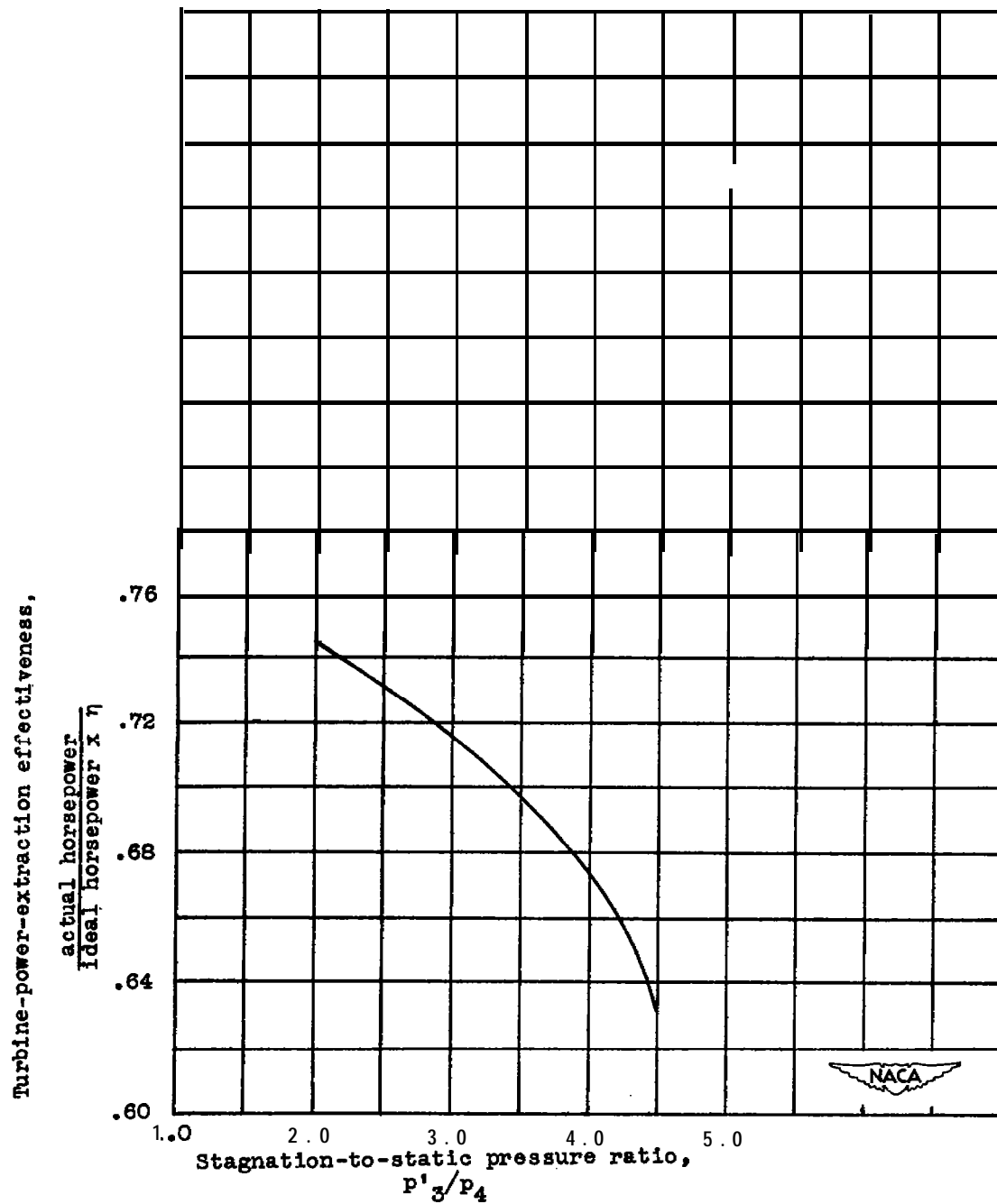


Figure 5. - Variation of turbine-power-extraction effectiveness with stagnation-to-static pressure ratio.

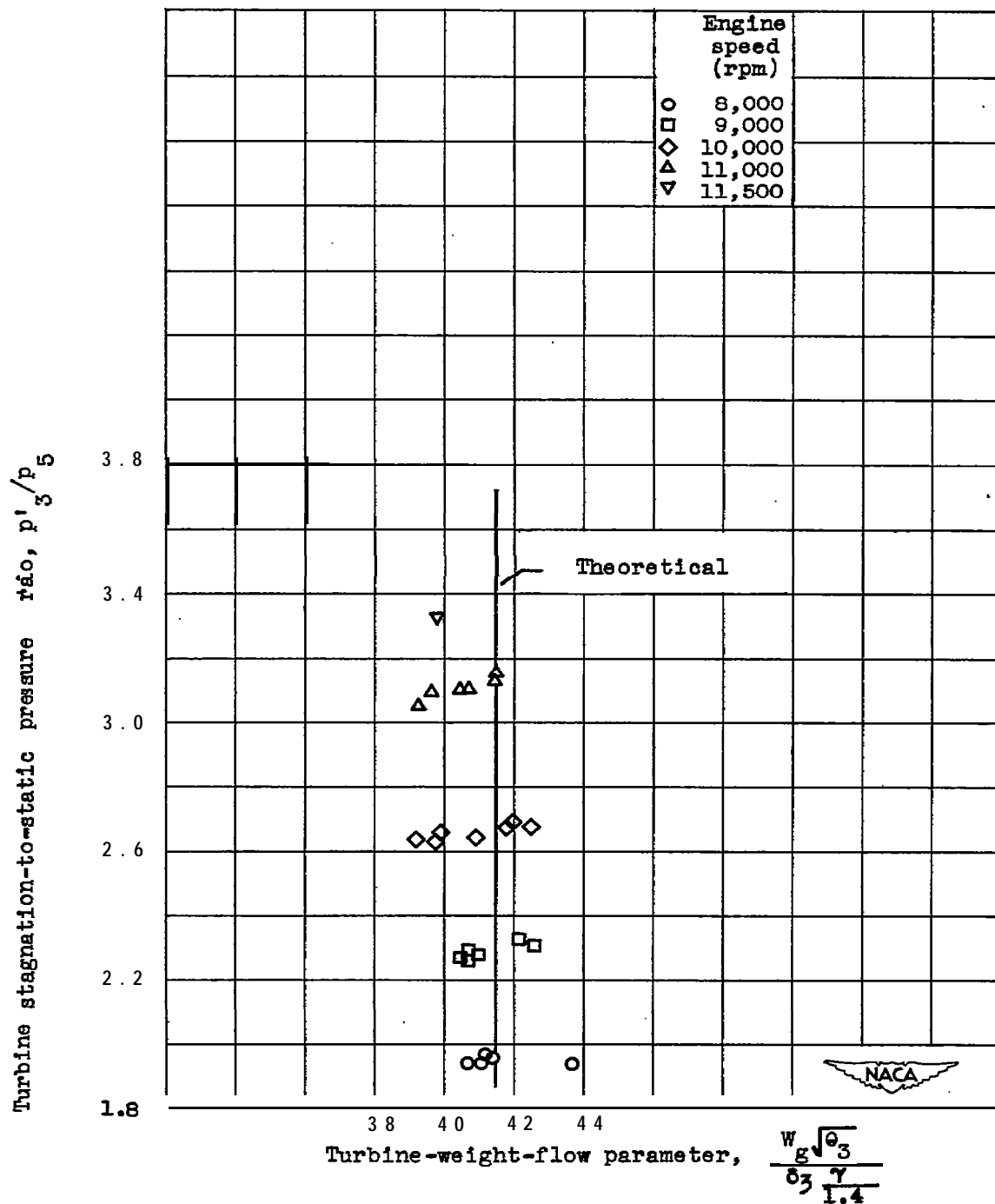


Figure 6. Variation of turbine-weight-flow parameter with stagnation-to-static pressure ratio. Jet-nozzle diameter, 2.0 inches.

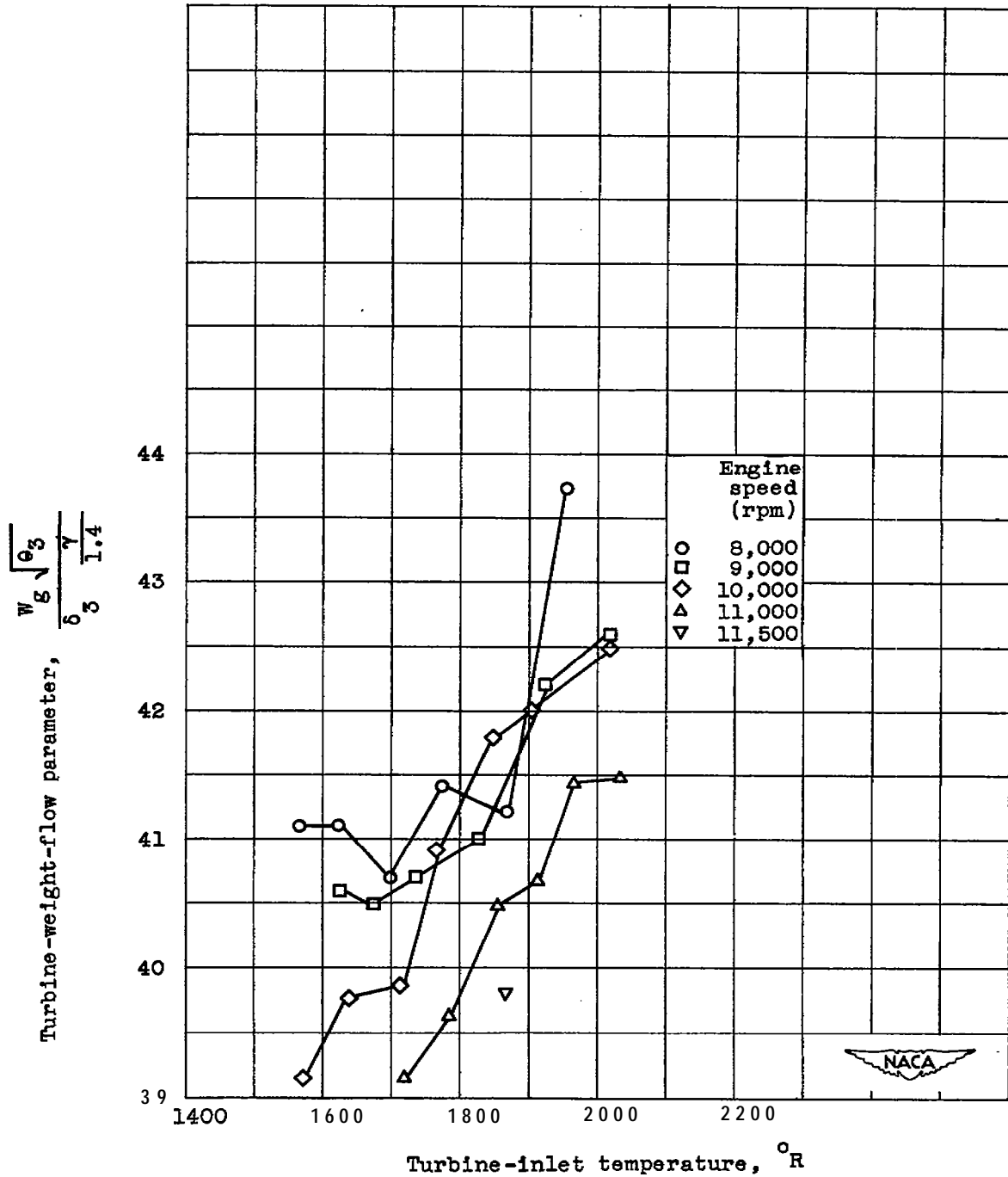


Figure 7. - Variation of turbine-weight-flow parameter with turbine-inlet temperature. Jet-nozzle diameter, 20 inches.

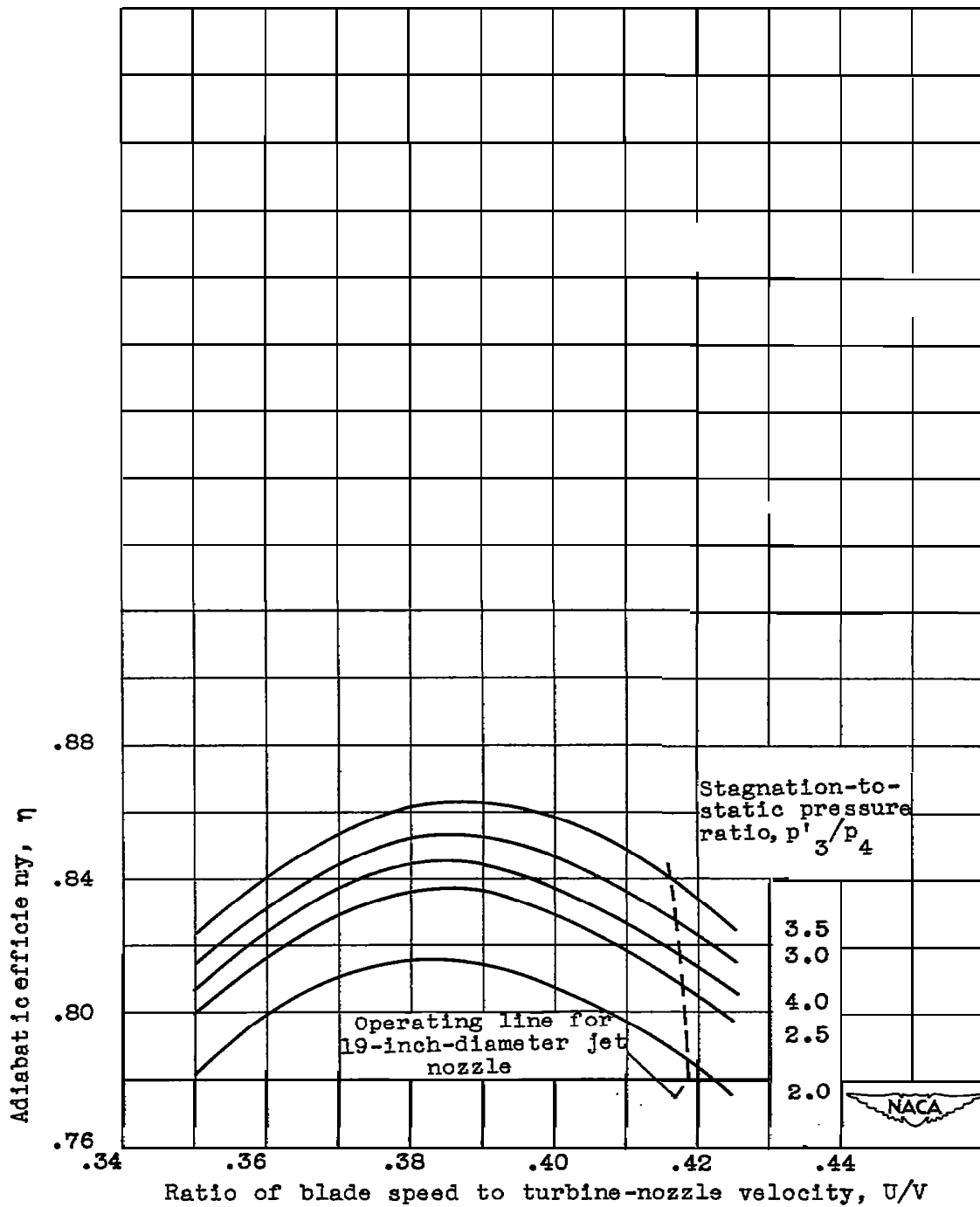


Figure 8. - Variation of adiabatic efficiency with ratio of blade speed to turbine-nozzle velocity.

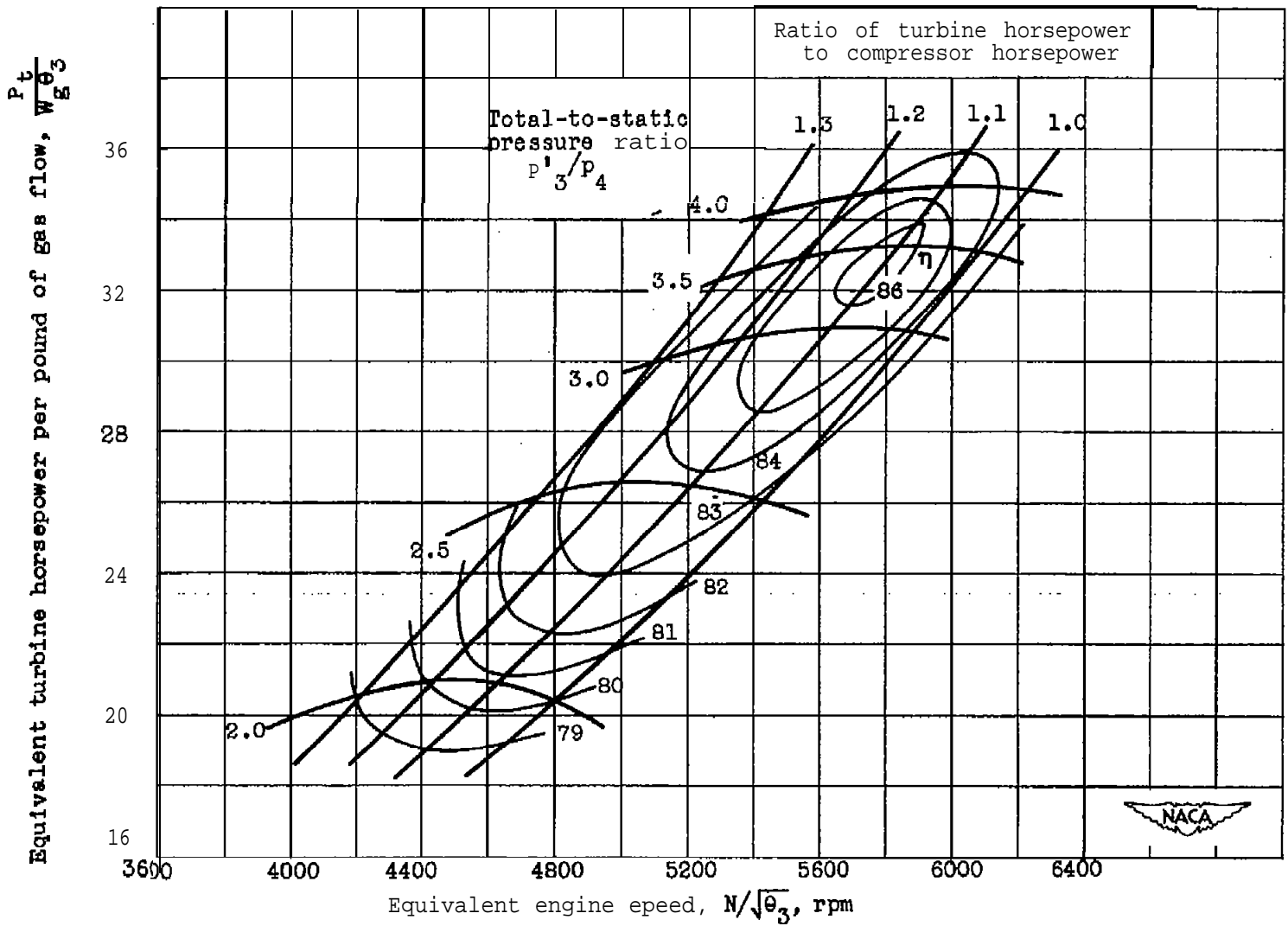


Figure 9. - Performance characteristic curves for turbine component.

NASA Technical Library



3 1176 01435 0756

